Photoluminescence of the $A^2\Pi - X^2\Sigma^+$ System of the Yttrium Oxide Molecule

C. LINTON

Physics Department, University of New Brunswick, Fredericton, New Brunswick, Canada E3B 5A3

A cw dye laser, tunable in the region 570–620 nm, has been used to excite photoluminescence in the $A^2\Pi-X^2\Sigma^+$ system of the YO molecule. Two methods have been used to obtain spectra. They are (*i*) photoluminescence and (*ii*) spectrally selective excitation spectroscopy. The latter maintains the simplicity of photoluminescence, but has higher resolution. The spectra obtained at medium resolution ($\sim$0.05 nm) have been surveyed and the identification of transitions has been outlined. A method was devised in which known lower state constants were used in calculating approximate upper state constants whenever the laser simultaneously excited coincident rotational transitions in the same band. From these calculations, an approximate value of α'_e was calculated which was found to be close to, but slightly larger than values previously computed from the Pekeris formula. Many examples of collisional transfer were observed. In particular, maximum transfer from $^2\Pi_{\frac{1}{2}}$ to $^2\Pi_{\frac{3}{2}}$ was always observed to involve an increase of one unit in the vibrational quantum number. No transfer was observed between opposite parity components of Λ doublets, in spite of their closeness in energy, indicating that the symmetry of the electronic eigenfunctions was unaffected by collisions. Reanalysis of previous high resolution data has shown that, when the contribution of Λ-doubling parameters to the separation of the $^2\Pi_{\frac{1}{2}}$ and $^2\Pi_{\frac{3}{2}}$ states is taken into account, the value of the spin–orbit coupling constant, A, changes significantly. It was also found necessary to include the constant, A_D, to account for the effect of centrifugal distortion on the spin–orbit interaction.

I. INTRODUCTION

A. The YO Spectrum

The spectrum of the yttrium oxide molecule is of importance to astrophysicists as it is a prominent feature in some M-type stars. It is also of interest to compare the YO spectrum with known spectra of isovalent molecules, e.g., CaF, SrF, BaF, ScO, LaO. In all of these molecules, $B^2\Sigma^+-X^2\Sigma^+$ and $A^2\Pi-X^2\Sigma^+$ systems have long been established (*1–3*). In ScO, LaO, and YO, a low-lying $A'^2\Delta$ state has been observed via a $C^2\Pi-A'^2\Delta$ transition in LaO (*4*) and $A'^2\Delta-X^2\Sigma^+$ transitions in ScO and YO (*5*). It was shown (*5*) that the intensity of the $A'^2\Delta-X^2\Sigma^+$ transitions arose as a result of mixing between the $A'^2\Delta$ and $A^2\Pi$ states. This mixing was shown to be considerable in the case of YO. So far all attempts to observe the equivalent $^2\Delta$ state in the group IIa halides have failed.

The $B–X$ and $A–X$ systems of YO lie in the blue–green and orange–red regions, respectively, and the $A'–X$ system is in the 620–747-nm region. Vibrational analyses have been performed on all these systems (*1, 5*) and the 0–0 bands of the $B–X$ and $A–X$ systems have been rotationally analyzed (*2*). In both of these systems, the band structure

is open and extensive and severe overlapping complicates analysis of bands from high vibrational levels.

A possible way of obtaining information about higher vibrational states ($v' > 0$) while avoiding problems caused by overlapping bands is to use laser-induced photoluminescence techniques. The $A-X$ system lies in a spectral region readily accessible to cw dye lasers (using Rhodamine 6G), and it was thus decided to investigate the possibilities of using this method as a means of gaining more detailed information about this system. This paper presents a survey of low resolution photoluminescence spectra obtained from the $A-X$ system, indicating the complexities of photoluminescence from this kind of transition and clearly showing the potential usefulness of high resolution experiments of this nature.

The $A-X$ systems of all the above isovalent molecules are very similar in structure. In YO, the $A-X$ system consists primarily of two strong sequences of bands, starting at 597.2 and 613.2 nm, and representing the $\Delta v = 0$ sequences originating from the $^2\Pi_{\frac{3}{2}}$ and $^2\Pi_{\frac{1}{2}}$ components, respectively. The $\Delta v = \pm 1$ transitions are very weak as the two potential curves lie vertically above each other. Rotational structure of the 0–0 band has been observed up to $N = 142$ and has been measured to the 4–4 bandhead. In their analysis, Uhler and Åkerlind (2) concluded that the spin splitting in the $X^2\Sigma^+$ state was negligible, the spin–orbit splitting in the $A^2\Pi$ state was 428 cm^{-1}, and that Λ doubling was very large in $^2\Pi_{\frac{1}{2}}$ and negligible in the $^2\Pi_{\frac{3}{2}}$ component. This is illustrated in Fig. 1 which shows the expected transitions for $^2\Pi$ (case a)–$^2\Sigma$ in the case where no

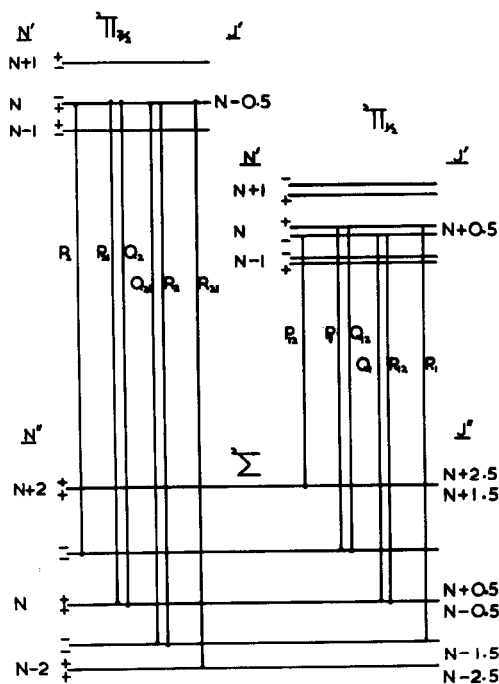FIG. 1. Energy levels and branches for a $^2\Pi$ (case a)–$^2\Sigma$ transition with no Λ doubling in the $^2\Pi_{\frac{3}{2}}$ state and negligible splitting in the $^2\Sigma$ state.

splitting is observed in either the $^2\Sigma$ or $^2\Pi_{\frac{1}{2}}$ states. The details of this type of transition have been discussed elsewhere (6, 7) and only a brief outline will be given here. Because of the small splitting in the X state, only four of the six possible branches in each subsystem will be observed, as there are four sets of coincident branches, $^QP_{21}$ and Q_2, $^RQ_{21}$ and R_2, P_1 and $^PQ_{12}$, Q_1 and $^QR_{12}$, which will subsequently be referred to as Q_2, R_2, P_1, and Q_1. Each subband ($^2\Pi_{\frac{3}{2}}$, $^2\Pi_{\frac{1}{2}}$) consists of two red-degraded band-heads, one very intense (R_2, Q_1) and a much weaker one ($^SR_{21}$, R_1) at shorter wavelengths. The latter heads are often difficult to observe as they form at much higher N values ($N_{\text{head}} \sim 240$) than the R_2 and Q_1 heads ($N_{\text{head}} \sim 80$). The $^SR_{21}$, P_2, R_1, and $^OP_{12}$ branches are easiest to resolve as the separation of the lines in these branches is approximately three times as great as that in the R_2, Q_2, Q_1, and P_1 branches (6).

B. Photoluminescence

As photoluminescence from the A–X system of CaF, which is very similar to that of YO, has been discussed in detail by Field et al. (7), only the main points relevant to this work will be discussed in this section.

In order to identify transitions observed in photoluminescence, several combination relations were used. From Fig. 1 it can be seen that, if the laser excites a single Λ-doubled component of a rotational level, there are two transitions that can take place from this level (three if the lower state splitting were resolved). The frequency difference between these two transitions is related to rotational energy spacings in the lower state. The following relations are obtained for emission lines from a common upper state, N.

(i) $^2\Pi_{\frac{3}{2}}$–$^2\Sigma$:

$$^SR_{21}(N - 2) - Q_2(N) = 4B''(N - \tfrac{1}{2}).$$ (1)

$$R_2(N - 1) - P_2(N + 1) = 4B''(N + \tfrac{1}{2}).$$ (2)

(ii) $^2\Pi_{\frac{1}{2}}$–$^2\Sigma$:

$$R_1(N - 1) - P_1(N + 1) = 4B''(N + \tfrac{1}{2}).$$ (3)

$$Q_1(N) - ^OP_{12}(N + 2) = 4B''(N + \tfrac{3}{2}).$$ (4)

These relations were used to determine N, as B'' is known from the rotational analysis (2).

The photoluminescence spectrum from a single excited level would therefore be expected to consist of a series of doublets with the separation of successive doublets representing vibrational spacings in the lower state.

C. Excitation Spectra

The degree of detail obtainable from photoluminescence spectra is dependent on the resolution of the spectrometer, i.e., the spectral slit width. An alternative method of studying the spectrum is to use the spectrometer as a monochromator, i.e., set it to detect a narrow wavelength range, and scan the laser through its tunable wavelength region. The spectrum obtained will be a plot of intensity against laser wavelength. A signal will only be obtained when the laser excites a state from which a transition can take place in the wavelength region for which the spectrometer is set. As the resolution is dependent on the laser linewidth and not on the spectrometer, this method enables

one to obtain high resolution spectra with a low resolution spectrometer. The effect of increasing the width of the spectrometer slit is to increase the number of accessible transitions and hence add more features to the spectrum without affecting resolution. This technique of spectrally selective excitation spectroscopy therefore combines the simplicity of photoluminescence spectroscopy with the resolution of excitation spectroscopy.

In the present experiment both techniques were used to study the YO molecule.

D. Calculation of Approximate Upper State B Values

If the laser excites two coincident rotational transitions in the same band, this information may be used to determine rotational constants of one state if those of the other state are known.

For a molecule like YO, in which the spin–orbit splitting of the $^2\Pi$ state is very large, the expressions for the rotational term values (6) of the $A\,^2\Pi$ state reduce to

$$F'_1(N) = B'N(N+2) - (A/2) - D'(N+\tfrac{1}{2})^4 \pm \tfrac{1}{2}p(N+1), \qquad (5)$$

$$F'_2(N) = B'(N^2 - 1) + (A/2) - D'(N+\tfrac{1}{2})^4, \qquad (6)$$

where A is the spin–orbit coupling constant, and p is the Λ-doubling constant.

For the ground state, with zero spin splitting, the rotational term values are given by

$$F''(N) = B''N(N+1) - D''N^2(N+1)^2. \qquad (7)$$

If, for example, the laser simultaneously excited rotational levels N_1 in a P_2 branch and N_2 in a Q_2 branch then, because of this coincidence, we may write

$$P_2(N_1 + 1) = Q_2(N_2),$$

$$F'_2(N_1) - F''(N_1 + 1) = F'_2(N_2) - F''(N_2).$$

Substitution of Eqs. (6) and (7) into this expression gives, to a first approximation,

$$B' = \frac{[N_2(N_2 + 1) - (N_1 + 1)(N_1 + 2)]}{[N_2{}^2 - N_1{}^2]}B''. \qquad (8)$$

Inclusion of terms in D' and D'' will add a small correction term (≤ 0.0003) to this expression. N_1 and N_2 are calculated from Eqs. (1) and (2) and if B'' is known, an approximate value can be calculated for B'.

A small error may occur in this calculation because of the possibility that the coincident lines may not have exactly the same frequency, but may have a small frequency difference which lies within the width of the exciting laser line. To overcome this, a second method, involving the second components in the photoluminescence spectrum, may also be used to calculate B'.

Excitation of $P_2(N_1 + 1)$ and $Q_2(N_2)$ will lead to emission of $R_2(N_1 - 1)$ and $^SR_{21}(N_2 - 2)$. By measuring the frequency separation, $\Delta\nu$, between these lines, the following expressions may be used:

$$\Delta\nu = {}^SR_{21}(N_2 - 2) - R_2(N_1 - 1)$$

$$= F'_2(N_2) - F''(N_2 - 2) - F'_2(N_1) + F''(N_1 - 1).$$

Substitution of Eqs. (6) and (7) into this expression gives, to a first approximation,

$$B' = \frac{\Delta\nu + B''[(N_2 - 2)(N_2 - 1) - (N_1 - 1)N_1]}{[N_2^2 - N_1^2]}. \tag{9}$$

A second value for B' may be calculated from this expression. If there is a large discrepancy between the values calculated from Eqs. (8) and (9), the values of N_1 and/or N_2 may be adjusted within their range of uncertainty (± 1 in this experiment) until consistent values are obtained for B'.

Similar expressions may be obtained for other possible coincident lines ($^S R_{21}$, R_2; $^O P_{12}$, P_1; R_1, Q_1). Calculations involving the $^2\Pi_{\frac{1}{2}}$ component will require knowledge of p, the Λ-doubling constant. The accuracy of the results depends on the resolution of the experiments and the accuracy of the lower state constants. However, even at the resolution of the present experiments, B values accurate to $\pm 5 \times 10^{-4}$ cm^{-1} or better can be obtained for $v' = 0$ to $v' = 2$ and will lead to experimental information about the value of α_e, which previously has only been calculated (2) using the Pekeris formula.

II. EXPERIMENTAL DETAILS

Details of the furnace apparatus have been described elsewhere (8). Yttrium metal was evaporated from a resistively heated graphite crucible and the vapor, entrained in a flow of cool argon gas, was carried into a reaction chamber to react with oxygen molecules, producing a bright red chemiluminescent flame at a crucible temperature of around 1800 K. Light from an Ar$^+$ pumped cw dye laser was directed vertically into the flame through a window at the top of the furnace. The laser, using Rhodamine 6G, could be continuously tuned and scanned in the region 570–620 nm. Multimode excitation was used, giving a bandwidth of $\sim$0.05 nm.

Spectra were recorded photoelectrically using a 1-m Czerny–Turner spectrometer. The spectrometer resolution was $\sim$0.05 nm for photoluminescence spectra while, for excitation spectra, the spectral slit width was between 0.05 and 0.20 nm.

III. REANALYSIS OF ROTATIONAL DATA

Since the original analysis by Uhler and Åkerlind (2), a great deal of improvement has been made in techniques for reducing molecular spectra to constants. One recent technique is the "Direct Approach" of Zare et al. (9) in which trial molecular constants are used to calculate the matrix elements of the upper and lower state effective Hamiltonians. The Hamiltonian matrices are then diagonalized, and calculated line positions are computed from the differences between the resulting upper and lower state eigenvalues. A least-squares technique is then used to adjust the molecular constants until satisfactory agreement is obtained between measured and calculated line positions.

It was decided to use this method to reanalyze Uhler and Åkerlind's (2) original data for several reasons. It has been shown (10, 11) that the separation between $^2\Pi_{\frac{1}{2}}$ and $^2\Pi_{\frac{3}{2}}$ states is not entirely due to the spin–orbit interaction but that there is also some contribution from Λ-doubling parameters. Especially important in this respect is the parameter, o, which cannot be determined independently of the band origin, ν_0, and the spin–orbit coupling constant, A. Because of this, its effects are usually absorbed into ν_0 and A with the result that quoted values usually do not represent the true values. Because

of its correlation with ν_0 and A, o has to be estimated independently by means of the unique perturber approximation (*9, 11*) which leads to the expression

$$o = (A/8B) \cdot p.$$

This neglects the effect of the known perturbation of $A^2\Pi$ by $A'^2\Delta$ (*5*) which, strictly speaking, should be considered in determining meaningful constants. However, as the pure precession estimate of the Λ-doubling constant, p, obtained assuming interaction only with $B^2\Sigma^+$, is in good agreement with experiment (*12*), it is expected that the calculated value of o will be reasonably accurate. As the Λ doubling, and hence p, is large for YO, then calculation of o is expected to have a significant effect on the values of ν_0 and A. Another reason for reanalysis is that, because lines of very high N were obtained, it is possible that a more complete treatment of centrifugal distortion effects should be taken into account in order to fit the observed lines.

The results of the analysis showed that the values of B', D', p', B'', and D'' were not significantly different from the quoted values. However, in order to fit the lines accurately, it was necessary to include centrifugal distortion effects in the spin–orbit interaction and compute the constant A_D (*9*). This improved the standard deviation of the fit by an order of magnitude. When all lines were used in the calculation, the constants (shown in Table I) reproduced the measured lines to within a standard deviation of 0.05 cm^{-1}. Although the calculated value of the separation of $^2\Pi_{\frac{1}{2}}$ and $^2\Pi_{\frac{3}{2}}$ remains unaltered, the effect of computing o can be seen when A is compared with the original value of 428.03 cm^{-1} (*2*). It was also found that a significant improvement to the fit was obtained by including the constant, p_D, representing the effect of centrifugal distortion on the Λ doubling.

IV. RESULTS

A. General

Very bright photoluminescence was observed at laser wavelengths corresponding to bandheads of the A–X system. Photoluminescence was continuously visible from

TABLE I

Revised Molecular Constants (in cm^{-1}) for the YO $A^2\Pi$–$X^2\Sigma^+$ System

Constant	$A^2\Pi$	$X^2\Sigma^+$
B	0.385776(53)	0.388092(54)
D	3.468(27) $\times$ 10^{-7}	3.188(28) $\times$ 10^{-7}
A	408.757(42)	
A_D	3.136(58) $\times$ 10^{-4}	
p	-0.14969(33)	
p_D	-2.27(38) $\times$ 10^{-7}	
o	-19.83 (calculated)	
	Origin: ν_o = 16518.984(22)	

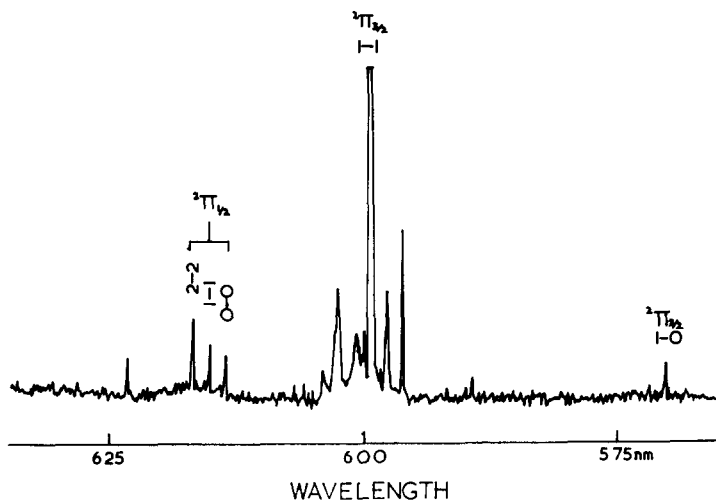Figures in parentheses represent the two standard deviation uncertainties in the final two digits.

FIG. 2. Photoluminescence spectrum of YO excited at a laser wavelength of 598.8 nm, close to the 1–1 bandhead ($^2\Pi_{\frac{1}{2}}$–$^2\Sigma$) at a total pressure of 7 Torr. The spectral slit width was 0.05 nm and the spectrum was scanned at a rate of 50 nm/min.

597–620 nm and was strongest at 597.22 and 613.21 nm, the heads of the $^2\Pi_{\frac{3}{2}}$ and $^2\Pi_{\frac{1}{2}}$ components of the 0–0 band. In this study, spectra were obtained of photoluminescence excited at the wavelengths of the 0–0, 1–1 (both components), and 2–2 ($^2\Pi_{\frac{1}{2}}$ component) bandheads. In addition, excitation spectra were obtained with the spectrometer set at these wavelengths. Spectra also were obtained of photoluminescence from various features of the 0–0 band (both components). In order to illustrate typical features, spectra of the 1–1 band ($^2\Pi_{\frac{1}{2}}$) will be discussed in detail. Results from other bands will also be presented.

B. 1–1 Band ($^2\Pi_{\frac{1}{2}}$–$^2\Sigma$)

(i) *Photoluminescence.* When the laser was set at a wavelength close to that of the R_2 head of the $^2\Pi_{\frac{1}{2}}$–$^2\Sigma$ component of the 1–1 band (598.8 nm), a bright orange photoluminescence was observed. The low resolution spectrum obtained at an argon pressure of 7 Torr is shown in Fig. 2. The spectrum is quite complex, consisting of several features between 596 and 604 nm on both sides of the laser line, a weak feature at 570 nm, and three bands of the $^2\Pi_{\frac{1}{2}}$–$^2\Sigma$ component between 613 and 619 nm. The feature at 570 nm is the 1–0 band and, apart from the 1–1 band, is the only band of the $v' = 1$ progression which appeared in the photoluminescence spectra. The very low intensity of this band was expected from the Franck–Condon factors and its banded structure arises because the laser excited many closely spaced lines around the bandhead. The complexity of the structure around the laser line suggests that the laser excited many coincident transitions. A higher resolution spectrum of this region (Fig. 3—upper spectrum), taken under the same experimental conditions, confirms this. The spectrum consists of single lines at 595.83, 597.55, and 599.54 nm, two sets of resolved rotational lines with peaks at 602.20 and 603.66 nm, and the 0–0 and 2–2 bandheads at 597.21 and 600.32 nm. In addition, the 0–0, 1–1, and 2–2 bands of the $^2\Pi_{\frac{1}{2}}$–$^2\Sigma$ component are shown. The dotted features
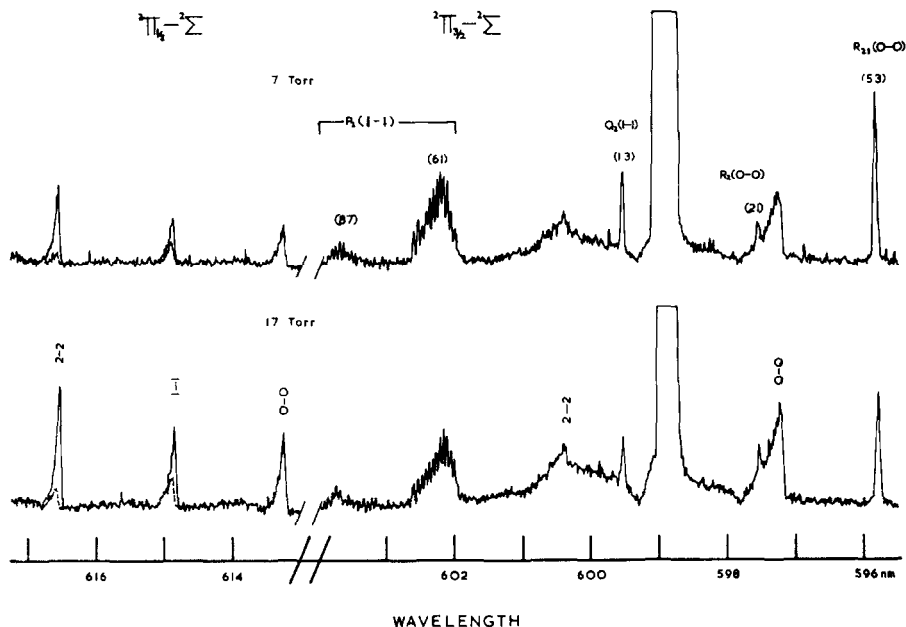
FIG. 3. Photoluminescence spectrum of YO excited at a laser wavelength of 598.8 nm, close to the 1–1 bandhead ($^2\Pi_{\frac{1}{2}}$–$^2\Sigma$), at total pressures of 7 Torr (top) and 17 Torr (bottom). The spectral slit width was 0.05 nm and the spectrum was scanned at a rate of 5 nm/min. The dotted features under the heads of 1–1 and 2–2 subbands ($^2\Pi_{\frac{1}{2}}$–$^2\Sigma$) represent chemiluminescent emission from the flame. The 0–0 ($^2\Pi_{\frac{1}{2}}$–$^2\Sigma$) emission is almost entirely chemiluminescence. Numbers in parentheses directly above spectral features are the upper state N values of the transitions.

which can be seen under the heads of the 1–1 and 2–2 subbands ($^2\Pi_{\frac{1}{2}}$) represent the chemiluminescent spectrum of the flame taken with the laser switched off and show that there is considerable photoluminescence from these bands. Almost the entire signal from the 0–0 subband was from chemiluminescence. Chemiluminescence from the $^2\Pi_{\frac{1}{2}}$–$^2\Sigma$ component was very weak and all the intensity in this region was from photoluminescence.

The lines in the figures are labeled by the branch followed by the band in parentheses. The numbers in parentheses above the lines are the N values of the upper state excited by the laser. This is not standard notation but, as it is the upper state quantum number that is of prime importance in laser spectroscopy, this notation enables one to see at a glance which level the laser is exciting.

The laser, when tuned close to the 1–1 bandhead, excites many lines in the head-forming R_2 branch, resulting in emission of many resolved lines of the P_2 branch between 602.0 and 603.9 nm. The two peaks in this branch indicate that the laser line was centered slightly to the long wavelength side of the bandhead with the result that rotational levels with $N < N_{\text{head}}$ and $N > N_{\text{head}}$ were excited whereas N_{head} was hardly excited at all. The values of N were initially calculated from Eq. (2) and were refined by using the method outlined in Section ID to give a consistent value for B'. The center of the minimum between the two peaks falls approximately at N_{head} showing that $N_{\text{head}} \sim 74$. The only other branch of the 1–1 band in the neighborhood of the R_2 head is $^SR_{21}$ whose lines are widely spaced. The laser thus excited only one line ($N' = 13$) of

this branch with resulting emission of the corresponding line of the Q_2 branch at 599.54 nm. The 1–1 head is also overlapped by the P_2 and Q_2 branches of the 0–0 band as can clearly be seen in the high resolution spectra of Ref. (2). The laser line excited $N = 21$ of the P_2 branch resulting in emission of the R_2 line at 597.55 nm. The P_2 lines are widely spaced and the low intensity of the R_2 line indicates that the coincidence with the peak of the laser line was not exact. The Q_2 lines are closer together and the chances of coincidence are much better as indicated by the intensity of the $^SR_{21}$ line ($N = 53$) at 595.83 nm, emitted as a result of excitation of the corresponding Q_2 line.

(ii) *Excitation spectrum.* When the spectrometer wavelength was fixed at the peak of the laser line used to excite the photoluminescence discussed above, and the laser was scanned through its spectral range, the excitation spectrum shown in Fig. 4 was obtained. When compared with the photoluminescence spectra (Fig. 3) it is apparent that the essential features are the same. Any slight differences occur because the spectral width of the laser line is smaller than that of the spectrometer slit. This results in (a) higher resolution in the excitation spectrum, (b) more lines in the P_2 branch of the 1–1 band as the spectral width of the spectrometer covers more lines of the R_2 branch including the head, (c) greater intensity in the R_2 ($N = 21$) line of the 0–0 band as the increased spectral width allows a better coincidence with the P_2 line, (d) several resolved lines in the $^SR_{21}$ branch of the 0–0 band as the spectral width now contains more lines of the Q_2 branch. Apart from the above, there are no fundamental differences between the photoluminescence and excitation spectra.

(iii) *Relaxation phenomena.* Not all the emission features observed in Fig. 3 can be explained on the basis of emission from the states excited directly by the laser, but must result from various collisional processes. Similar experiments with other molecules (BaO, TiO) have shown clear evidence of vibrational and rotational relaxation (13) and transfer between two electronic states of similar energy (14).

As the pressure was increased from 7 to 17 Torr (Fig. 3), the intensities of the banded features all increased relative to those of the sharp lines, indicating that the bands all resulted from collisional processes. In the $^2\Pi_{\frac{1}{2}}-^2\Sigma$ system, collisional effects are most
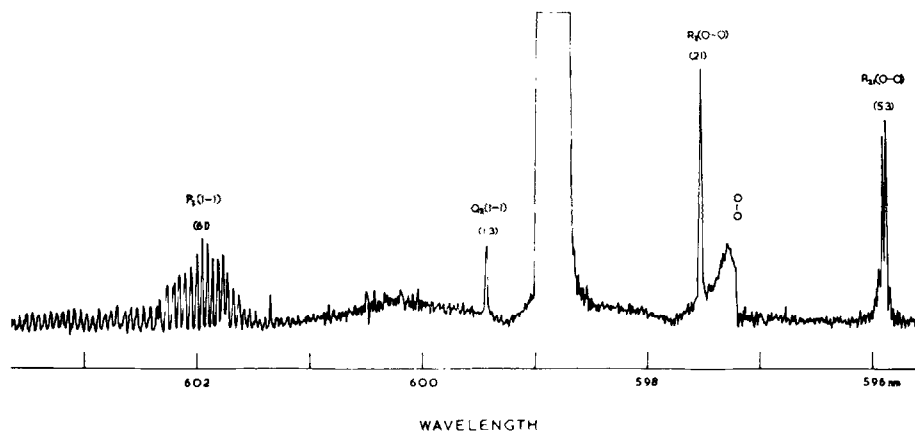

FIG. 4. Excitation spectrum of YO taken at a spectrometer setting of 598.8 nm, close to the 1–1 bandhead ($^2\Pi_{\frac{1}{2}}-^2\Sigma$), at a total pressure of 7 Torr and spectral slit width of 0.05 nm. Numbers in parentheses directly above spectral features are the upper state N values of the transitions.

noticeable in the 0–0 band at 597.21 nm. At 17 Torr the intensity of the head is comparable with that of the laser-induced lines. The 2–2 bandhead, which is much weaker, also increased in intensity at higher pressure. In addition to changing the vibrational and rotational states of some molecules, collisions also induce changes in the spin–orbit component and transfer some molecules from the $^2\Pi_{\frac{3}{2}}$ to the $^2\Pi_{\frac{1}{2}}$ state. This is responsible for photoluminescence from the 0–0, 1–1, and 2–2 bands of the $^2\Pi_{\frac{1}{2}}$–$^2\Sigma$ transition. When the background chemiluminescence is subtracted from the total signal, it is seen that the 2–2 band has the greatest intensity, there is significant emission from the 1–1 band, and very little from the 0–0 band. This indicates that the most efficient transfer is $^2\Pi_{\frac{3}{2}}$ ($v = 1$) $\rightarrow$ $^2\Pi_{\frac{1}{2}}$ ($v = 2$). There is noticeable transfer to $v = 1$, very little to $v = 0$, and none to $v > 2$. This is expected from energy considerations. Because of the large spin–orbit splitting, the states excited in $^2\Pi_{\frac{3}{2}}$, $v = 1$ are closer in energy to those forming the head in $^2\Pi_{\frac{1}{2}}$, $v = 2$ than they are to the head forming states in $^2\Pi_{\frac{1}{2}}$, $v = 1$. The energy match with $^2\Pi_{\frac{1}{2}}$, $v = 0$ is poor and is worse for $v > 2$. Similar effects were observed when the laser was tuned to other heads of the $^2\Pi_{\frac{3}{2}}$–$^2\Sigma$ system. In each case, excitation of ($^2\Pi_{\frac{3}{2}}$, v) resulted in maximum intensity from ($^2\Pi_{\frac{1}{2}}$, $v + 1$).

In spite of their closeness in energy, there was no evidence of any transfer between the opposite parity components of Λ doublets. In the $^2\Pi_{\frac{3}{2}}$ component, rotational analysis failed to resolve any Λ doubling (2) indicating that the components are separated by less than 0.03 cm^{-1}. However, excitation of lines in (say) the R_2 branch resulted only in emission from the component excited (R_2 and P_2) and not from the other component ($^SR_{21}$ and Q_2). This appeared quite rigorous under all conditions and shows that the electronic eigenfunctions were not affected by collisions.

C. Other Bands

The spectra shown in Figs. 3 and 4 are typical of the photoluminescence and excitation spectra of this system and illustrate how this technique can be used to obtain resolved rotational structure of bands that, in conventional sources, would be heavily overlapped by other bands. Further examples in Figs. 5–7 show excitation spectra obtained when the spectrometer was set on various features of the $^2\Pi_{\frac{3}{2}}$–$^2\Sigma$ 0–0 band, and illustrate typical differences in spectra obtained at wavelengths close to the head, close to the origin, and far away from the head of a single band.

In Fig. 5, the spectrometer was set at the bandhead wavelength. At this position, the only possible overlap is with the $^SR_{21}$ branch of the 1–1 band. Figure 6 shows the excitation spectrum obtained when the spectrometer was set on one of the more intense resolved lines of the P_2 branch (Fig. 5). As this wavelength is in a region covered by the 0–0, 1–1, 2–2, and 3–3 bands, several coincidences are expected. The spectrum clearly shows this overlapping. Figure 7 shows an excitation spectrum for low N values of the 0–0 band. The spectrometer was set slightly to the long wavelength side of the band origin, corresponding to low N lines of the P_2 and Q_2 branches, and also to one line of the $^SR_{21}$ branch of the 1–1 band. In all the above spectra, the rotational structure of P_2 and $^SR_{21}$ branches was resolved. Spectra of other bands originating from both $^2\Pi_{\frac{1}{2}}$ and $^2\Pi_{\frac{3}{2}}$ components were similar to those shown. At all laser wavelengths, at least three transitions were excited and, in general, the further away (to the red) the laser wavelength was from the 0–0 bandhead, the more coincidences there were at any wavelength.
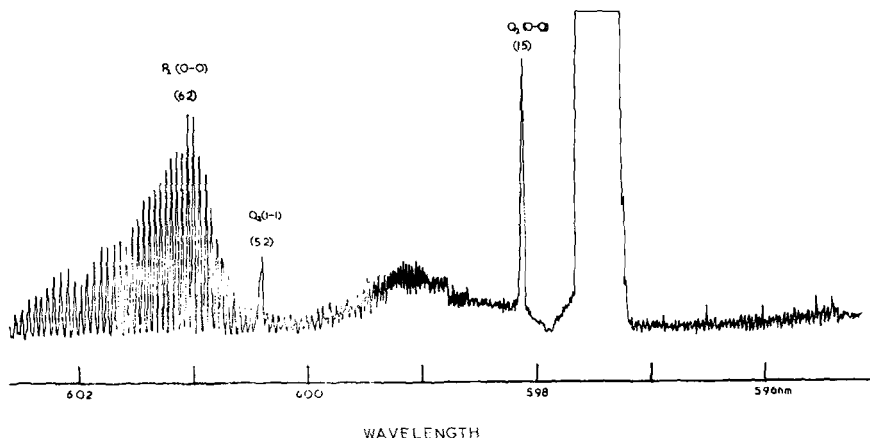
FIG. 5. Excitation spectrum of YO taken at a spectrometer setting of 597.2 nm, close to the 0–0 band-head ($^2\Pi_{\frac{1}{2}}$–$^2\Sigma$), at a total pressure of 6 Torr and spectral slit width of 0.05 nm. Numbers in parentheses directly above spectral features are the upper state N values of the transitions.

This emphasizes the extremely high density of lines in the spectrum and the difficulty of using conventional spectroscopy to obtain rotational data for transitions with $v' > 0$. A complete list of transitions excited in the present experiments is given in Table II. Features (usually bandheads) not mentioned in Table II were caused by rotational and vibrational relaxation.

D. Discussion

When suitable coincidences were found, the methods outlined in Section ID were used to calculate approximate B values for the $A^2\Pi$ state. Ground state rotational constants calculated by Uhler and Åkerlind (2) were used in the calculations, including their
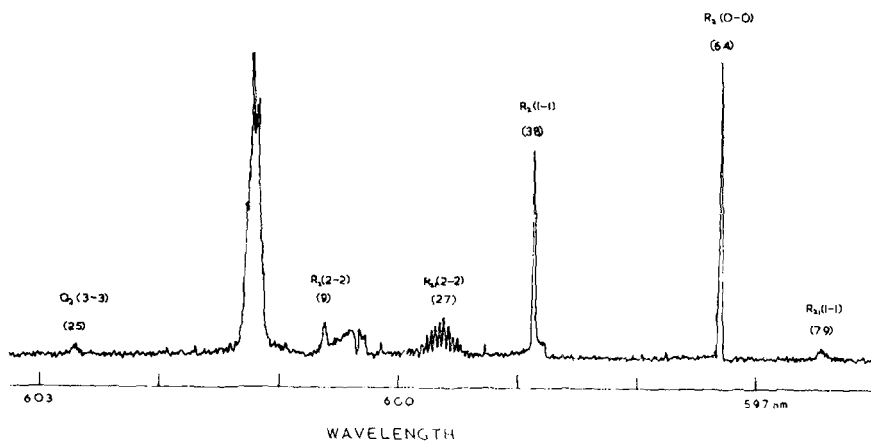

FIG. 6. Excitation spectrum of YO taken at a spectrometer setting of 501.2 nm, a total pressure of 6 Torr, and spectral slit width of 0.15 nm. Numbers in parentheses directly above spectral features are the upper state N values of the transitions.
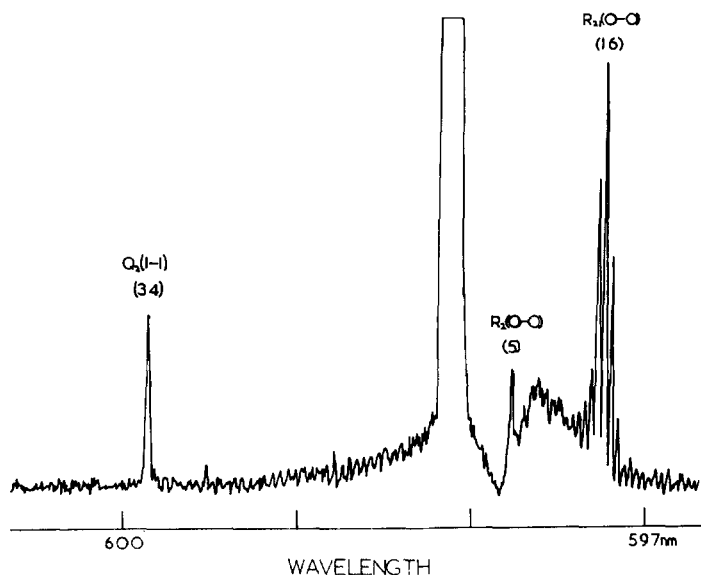
FIG. 7. Excitation spectrum of YO taken at a spectrometer setting of 598.1 nm, a total pressure of 6 Torr, and spectral slit width of 0.05 nm. Numbers in parentheses directly above spectral features are the upper state N values of the transitions.

value of $\alpha_e = 0.0016$ cm^{-1} which they estimated using the Pekeris formula. For the $^2\Pi_{\frac{1}{2}}$ state, it was assumed that the Λ-doubling constant, p, did not vary with v and the measured (2) value, $p = 0.151$ cm^{-1}, was used. Small corrections were applied to take into account effects of centrifugal distortion and the quoted values of D (2) were used. For each coincidence, values of N were calculated (Eqs. (1)–(4)) and then varied (by not more than one unit) until a pair was found that yielded consistent values of B' from Eqs. (8) and (9). It was found that the value of B' calculated for $^2\Pi_{\frac{3}{2}}$ was consistently ~ 0.0008 cm^{-1} higher than that calculated for $^2\Pi_{\frac{1}{2}}$. Equations (5) and (6) are approximations and require small correction terms (11). Calculation showed that these terms account for the observed difference of 0.0008 cm^{-1} between the two values of B'. However, the differences between B values for successive vibrational states, α_e, were constant for each component and the following values were obtained:

$$^2\Pi_{\frac{3}{2}}: B_0 - B_1 = 0.0022 \text{ cm}^{-1};$$

$$^2\Pi_{\frac{1}{2}}: B_0 - B_1 = 0.0019 \text{ cm}^{-1}; \quad B_1 - B_2 = 0.0020 \text{ cm}^{-1}.$$

The following average values were obtained.

$$B'_e = 0.3868 \pm 0.0005 \text{ cm}^{-1}; \quad \alpha'_e = 0.0020 \pm 0.0004 \text{ cm}^{-1}.$$

The transitions used in the calculations are marked (*) in Table II.

The accuracy of the above values naturally depends on that of the various constants used in the calculations. However, these preliminary experiments have indicated that, if the Pekeris value of α''_e is assumed to be correct, then the Pekeris value of α'_e (2) is probably slightly lower than the value determined here, but lies within the present

TABLE II

Transitions of the $A^2\Pi-X^2\Sigma^+$ System of YO Excited at Various Dye Laser Wavelengths

Exciting Wavelength (nm)	v'	v''	Branch Excited	Emitted	N'(Peak)**	Comments
597.2† (Fig. 5)	0	0	R_2	P_2	62	~50 lines
	0	0	$^SR_{21}$	Q_2	15	
	1	1	$^SR_{21}$	Q_2	52	
601.2 (Fig. 6)	0	0	P_2	R_2	64	
	1	1	Q_2	$^SR_{21}$	79	
	1	1	P_2	R_2	38	
	2	2	Q_2	$^SR_{21}$	27	~10 lines
	2	2	P_2	R_2	9	
	3	3	$^SR_{21}$	Q_2	25	
598.1 (Fig. 7)	*0	0	Q_2	$^SR_{21}$	16	
	*0	0	P_2	R_2	5	
	1	1	$^SR_{21}$	Q_2	34	
598.8† (Fig. 3)	*1	1	R_2	P_2	61	~12 lines
	*1	1	R_2	P_2	87	~ 9 lines
	*1	1	$^SR_{21}$	Q_2	13	
	*0	0	Q_2	$^SR_{21}$	53	
	*0	0	P_2	R_2	21	
613.2†	*0	0	Q_1	$^OP_{12}$	51	~30 lines
	*0	0	R_1	P_1	8	
	1	1	R_1	P_1	47	
616.1	0	0	$^OP_{12}$	Q_1	48	
	*1	1	P_1	R_1	53	~10 lines
	*1	1	$^OP_{12}$	Q_1	18	
	2	2	R_1	P_1	15	
	3	3	R_1	P_1	62	
614.8†	1	1	Q_1	$^OP_{12}$	45	~20 lines
	1	1	R_1	P_1	6	
	0	0	P_1	R_1	68	~ 6 lines
	0	0	$^OP_{12}$	Q_1	25	
616.5†	*2	2	Q_1	$^OP_{12}$	33 ⎫	2 peaks
	*2	2	Q_1	$^OP_{12}$	54 ⎭	separated
	*2	2	R_1	P_1	4	by minimum
	1	1	P_1	R_1	68	
	1	1	$^OP_{12}$	Q_1	26	
	0	0	$^OP_{12}$	Q_1	54	

† Laser or Spectrometer set at band head.
* Transitions used in calculations of B'.
** Accuracy = ±1 for transitions marked *, ±2 for others.

experimental uncertainty. The above value of α'_e is in good agreement with some very recent work by Bacis *et al.* (*15*), who have rotationally analyzed several bands of the YO molecule at very high resolution using a Fourier transform spectrometer.

These experiments have shown that, even at relatively low resolution, the photo-luminescence technique can provide new rotational information on the YO molecule. At higher resolution, much more detailed information should be obtainable. By studying photoluminescence using a high resolution spectrograph and moving the exciting wavelength in small steps through a band, it should be possible to perform a complete rotational analysis of vibrationally excited bands without encountering severe overlap problems. Alternatively, the same results could be attained with a low resolution spectrograph by recording excitation spectra using the laser in single mode operation. By setting the laser on perturbed lines (*2*) it may be possible to obtain information about the perturbing states. Because of the ease in observing collisionally induced

transitions in photoluminescence, it should be possible to make a more detailed study of collision processes in the flame.

This survey has shown that, although photoluminescence spectra of the $A^2\Pi-X^2\Sigma$ system of YO are fairly complex, the technique can provide a lot of new information about this molecule. Work is continuing along these lines with the hope of providing detailed rotational data on states up to $v = 10$.

RECEIVED: July 12, 1977

REFERENCES

1. L. W. JOHNSON AND R. C. JOHNSON, *Proc. Roy. Soc. Ser. A* **133**, 207 (1931).
2. U. UHLER AND L. ÅKERLIND, *Ark. Fys.* **19**, 1 (1961).
3. B. ROSEN, Spectroscopic data relative to diatomic molecules, *in* "International Tables of Selected Constants," Pergamon, New York, 1970.
4. D. W. GREEN, *J. Mol. Spectrosc.* **38**, 155 (1971).
5. C. L. CHALEK AND J. L. GOLE, *Chem. Phys.* **19**, 59 (1977).
6. G. HERZBERG, "Molecular Spectra and Molecular Structure: I. Spectra of Diatomic Molecules," Van Nostrand–Reinhold, New York, 1950.
7. R. W. FIELD, D. O. HARRIS, AND T. TANAKA, *J. Mol. Spectrosc.* **57**, 107 (1975).
8. J. B. WEST, R. S. BRADFORD, JR., J. D. EVERSOLE, AND C. R. JONES, *Rev. Sci. Instrum.* **46**, 164 (1975).
9. R. N. ZARE, A. L. SCHMELTEKOPF, W. J. HARROP, AND D. L. ALBRITTON, *J. Mol. Spectrosc.* **46**, 37 (1973).
10. R. S. MULLIKEN AND A. CHRISTY, *Phys. Rev.* **38**, 87 (1934).
11. T. C. JAMES, *J. Chem. Phys.* **41**, 631 (1964).
12. R. A. BERG, L. WHARTON, W. KLEMPERER, A. BÜCHLER, AND J. L. STAUFFER, *J. Chem. Phys.* **43**, 2416 (1965).
13. K. SAKURAI, S. E. JOHNSON, AND H. P. BROIDA, *J. Chem. Phys.* **52**, 1625 (1970).
14. C. LINTON AND H. P. BROIDA, *J. Mol. Spectrosc.* **64**, 389 (1977).
15. R. BACIS, A. BERNARD, AND P. LUC, Private communication and paper delivered at the "32nd Symposium on Molecular Spectroscopy," Columbus, Ohio, 1977.